

Ultraluminous X-ray bursts in two ultracompact companions to nearby elliptical galaxies

Jimmy A. Irwin¹, W. Peter Maksym², Gregory R. Sivakoff³, Aaron J. Romanowsky^{4,5}, Dacheng Lin⁶, Tyler Speegle¹, Ian Prado¹, David Mildebrath¹, Jay Strader⁷, Jifeng Liu^{8,9}, Jon M. Miller¹⁰

October 20, 2016

¹Department of Physics and Astronomy, University of Alabama, Box 870324, Tuscaloosa, Alabama, 35487, USA. ²Harvard-Smithsonian Center for Astrophysics, 60 Garden St., Cambridge, MA 02138, USA. ³Department of Physics, University of Alberta, CCIS 4-181, Edmonton, AB T6G 2E1, Canada ⁴Department of Physics & Astronomy, San José State University, One Washington Square, San Jose, CA 95192, USA. ⁵University of California Observatories, 1156 High Street, Santa Cruz, CA 95064, USA ⁶Space Science Center, University of New Hampshire, Durham, NH 03824, USA. ⁷Department of Physics and Astronomy, Michigan State University, East Lansing, MI 48824, USA. ⁸Key Laboratory of Optical Astronomy, National Astronomical Observatories, Chinese Academy of Sciences, 20A Datun Rd, Chaoyang District, Beijing, China 100012 ⁹College of Astronomy and Space Sciences, University of Chinese Academy of Sciences, 19A Yuquan Road, Beijing 100049, China ¹⁰Department of Astronomy, The University of Michigan, 1085 South University Avenue, Ann Arbor, Michigan, 48103, USA.

An X-ray flaring source was found near the galaxy NGC 4697¹. Two flares were seen, separated by four years. The flux increased by a factor of 90 on a timescale of about one minute. Both flares were very brief. There is no optical counterpart at the position of the flares¹, but if the source was at the distance of NGC 4697, the luminosities were $> 10^{39}$ erg s⁻¹. Here we report the results of a search of archival X-ray data for 70 nearby galaxies looking for similar such flares. We found two flaring sources in globular clusters or ultra-compact dwarf companions of parent elliptical galaxies. One source flared once to a peak luminosity of 9×10^{40} erg s⁻¹, while the other flared five times to 10^{40} erg s⁻¹. All of the flare rise times were < 1 minute, and they then decayed over about an hour. When not flaring, the sources appear to be normal accreting neutron star or black hole X-ray binaries, but they are located in old stellar populations, unlike the magnetars, anomalous X-ray pulsars or soft gamma repeaters that have repetitive flares of similar luminosities.

One source (hereafter Source 1) is located at RA=12:42:51.4, Dec=+02:38:35 (J2000) near the Virgo

elliptical galaxy NGC 4636 ($d = 14.3$ Mpc)^{2,3}. The cumulative X-ray photon arrival time plot and a crude background-subtracted light curve for this source derived from a $\sim 76,000$ second *Chandra* observation taken on 2003 February 14 are shown in Figure 1. Prior to and after the flare, the X-ray count rate of the source was $2.1 \pm 0.2 \times 10^{-3}$ counts s⁻¹ corresponding to a 0.3–10 keV luminosity of $7.9 \pm 0.8 \times 10^{38}$ erg s⁻¹ for a power law spectral model with a best-fit photon index of $\Gamma = 1.6 \pm 0.3$ (see *Methods*) if the source is at the distance of NGC 4636. About 12,000 seconds into the observation, the source flared dramatically, with six photons detected in a 22 second span, leading to a conservative peak flare count rate of $0.3^{+0.2}_{-0.1}$ counts s⁻¹, a factor of 70–200 increase in emission over its persistent (non-flare) state. Assuming the same spectral model as in the persistent state, the flare peaks at $9^{+6}_{-4} \times 10^{40}$ erg s⁻¹. Following the initial 22 second burst, the source emitted at a less intense but still elevated rate for the next 1,400 seconds. In total, 25 photons were emitted during the flare, for an average X-ray luminosity of $7 \pm 2 \times 10^{39}$ erg s⁻¹, and a total flare energy of $9 \pm 2 \times 10^{42}$ erg. We assess the probability of this burst being due to a random Poisson fluctuation of the persistent count rate is $\sim 6 \times 10^{-6}$ (see *Methods*). While the photon statistics during the 25-photon burst were limited, there was no evidence that the spectrum of the source differed during the flare. There are no apparent flares in the combined 370,000 seconds of the other *Chandra* and *XMM Newton* observations of NGC 4636, both before or after 2003 February 14 (see Extended Data Table 1).

A previous study⁴ associated Source 1 spatially with a purported globular cluster of NGC 4636 identified through Washington *C* and Kron-Cousins *R* system CTIO Blanco Telescope imaging⁵. While faint ($R=23.02$), the optical source identified as CTIO ID 6444 had a $C - R = 1.94$ color consistent with a globular cluster of near-solar metallicity⁵. Follow-up spectroscopic observations⁶ of a sub-sample of the globular cluster candidates in the vicinity of the globular cluster hosting Source

I found that 52/54 (96%) of the objects with a $C - R$ color and magnitude similar to CTIO ID 6444 were confirmed to be globular clusters of NGC 4636, with the two remaining objects identified as foreground Galactic stars. The hard X-ray spectrum of Source 1 during its persistent phase (see *Methods*) argues against it being a late-type Galactic dwarf star, for which the X-ray emission tends to be quite soft. Galactic RS CVn stars exhibit hard X-ray emission in quiescence and are known to undergo X-ray flares, but RS CVn have much higher optical-to-X-ray flux ratios⁷ compared to Source 1. Thus, it is highly likely that the optical counterpart of Source 1 is a globular cluster within NGC 4636. Based on its absolute R magnitude and $M/L = 4.1$, we estimate the globular cluster to have a mass of $3 \times 10^5 M_{\odot}$ (see *Methods*).

A second X-ray source located near the elliptical galaxy NGC 5128 showed similar flaring behavior. In the 2007 March 30 *Chandra* observation of NGC 5128, a source at RA=13:25:52.7, Dec=-43:05:46 (J2000; hereafter Source 2) began the observation emitting at a count rate of $9.5 \pm 1.5 \times 10^{-4}$ counts s^{-1} corresponding to a 0.3–10 keV luminosity of $4.4 \pm 0.7 \times 10^{37}$ erg s^{-1} using the best-fit $\Gamma = 1.0 \pm 0.2$ power law photon index and a distance⁸ of 3.8 Mpc for NGC 5128. Midway through the observation, the source flared dramatically, with 10 photons detected in a 51 second time span corresponding to a conservative peak luminosity estimate of $9_{-3}^{+4} \times 10^{39}$ erg s^{-1} , after which the flare subsided. Following the flare, Source 2 returned to its pre-flare luminosity for the remainder of the observation.

Inspection of other archival *Chandra* and *XMM-Newton* data (see Extended Data Table 1) revealed four more flares of Source 2. Three were observed with *Chandra* on 2007 April 17, 2007 May 30, and 2009 January 4, respectively, while the fourth flare was observed with *XMM-Newton* on 2014 February 9. In each instance, during the initial fast (<30 seconds) rise of the flare the count rate increased by a factor of 200–300 over the persistent count rate to $\sim 10^{40}$ erg s^{-1} , after which the flare subsided. The total flare energy of each of the five flares was $\sim 10^{42}$ erg. The light curves for the four *Chandra* flares look remarkably similar, as illustrated in Figure 2. We combined these four light curves into a combined background-subtracted light curve (see *Methods* for details) in Figure 2. Following the fast rise of the source by a factor ~ 200 to a peak luminosity approaching 10^{40} erg s^{-1} , the source remained in a roughly steady ultraluminous state for ~ 200 seconds before decaying over a time span of $\sim 4,000$ seconds (Figure 2). Fitting a power law to the combined spectra of the four *Chandra* flares yielded a best-fit photon index of $\Gamma = 1.2 \pm 0.3$. Thus, much like Source 1, the spectrum of Source 2 did not change appreciably during the flare.

Source 2 has been previously identified with the object HGH-C21 (also called GC 0320) within NGC 5128^{9–11}. With a spectroscopically-determined recessional velocity¹⁰ (460 km s^{-1}) within 110 km s^{-1} of NGC 5128, the source is clearly at the distance of NGC 5128. This implies a projected half-light radius¹² of 7 pc. With a velocity dispersion of 20 km s^{-1} and an inferred stellar mass¹² of $3.1 \times 10^6 M_{\odot}$, the optical counterpart is either a massive globular cluster or, given its unusual

elongated shape, more likely an ultracompact dwarf companion galaxy of NGC 5128.

It is unlikely that the flaring and the steady emission in both sources can be attributed to two unrelated sources in the same host. Since our flare search technique would have found these flares had they been detected by their flare photons alone, we can calculate the probability that these globular clusters would have also hosted steady X-ray emission more luminous than the persistent emission in each globular cluster (see *Methods*). The globular cluster in Source 1 has a <0.3% probability of having an X-ray source with a luminosity more than 8×10^{38} erg s^{-1} , while the globular cluster/ultracompact dwarf in Source 2 has a <9% probability of having an X-ray source with a luminosity more than 4×10^{37} erg s^{-1} . Multiplying these probabilities leads to only a <0.02% chance that both flares are unrelated to the steady emission. Of course, in the unlikely event that the flares are distinct sources from the persistent sources, the flaring sources must be flaring by more than two orders of magnitude over whatever their true non-flare luminosities are.

Summing up all the available archival *Chandra* and *XMM-Newton* data (but omitting the *Chandra* HRC and transmission grating exposures, which are not sensitive enough to detect a flare of similar intensity seen in the ACIS observations) allows us to constrain the duty cycle and recurrence rate of the flares. Source 2 flared five times for a total combined flare time of $\sim 20,000$ seconds in a total observation time of 7.9×10^5 seconds, yielding one flare every ~ 1.8 days and a duty cycle of $\sim 2.5\%$. Source 1 flared once for 1,400 seconds in a total observation time of 370,000 seconds. This single flare implies a recurrence timescale of >4 days and duty cycle of $<0.4\%$.

In terms of energetics, variability, and survivability, only short and intermediate duration soft gamma repeaters (SGRs)¹³ and their cousins the anomalous X-ray pulsars (AXPs)¹⁴ are comparable to the sources discussed here. However, SGRs/AXPs are believed to be very young and highly magnetized neutron stars, which would not likely be found in an old stellar population such as a globular cluster or red ultracompact dwarf galaxy. Our sources are also unlike SGRs/AXPs in that SGR/AXP flares of this magnitude only last a few to a few tens of seconds^{15,16} without an hour long decay as seen in our sources. Our sources are also unlikely to be Type II X-ray bursts of neutron stars, believed to result from rapid spasmodic accretion onto the neutron star. In addition to having flare-to-pre-flare luminosity ratios of only 10–20, the only Type II burst to reach 10^{40} erg s^{-1} (GRO 1744-28 – the Bursting Pulsar) exhibits several sub-minute flares per day when flaring, with much lower total flare energies per burst than our sources and different timing properties from our sources¹⁷. Furthermore, the quiescent X-ray luminosity of the Bursting Pulsar is 4–5 orders of magnitude fainter than the long-term luminosities of our sources. Qualitatively, the fast rise–slower decay of Source 2 (Figure 2) resembles that of Type I bursts from Galactic neutron stars, which typically peak near the Eddington limit of a neutron star. However, the peak luminosities from Sources 1 and 2 are 1–2 orders of magnitude greater than the Type I limit for even helium accretion, and last more than an order of magnitude

longer. Rare superbursts from Galactic neutron stars have been known to last for an hour^{18,19} but also have peak luminosities well below those of our sources. Other X-ray flares of unknown source published in the literature^{20–22} appear to be one-time transient events, indicating that they were (most likely) cataclysmic events with no post-flare emission, unlike our sources.

We have investigated the light curves of several thousand X-ray point sources within 70 *Chandra* observations of nearby galaxies and found only these two examples. It would appear that the Milky Way has no analogs to our sources. Given the number of X-ray sources in the Milky Way brighter than 10^{37} erg s⁻¹ (~ 40)²³, the lack of X-ray binaries more luminous than 10^{38} ergs s⁻¹ in Galactic globular clusters, and the rarity of burst sources in the extragalactic sample, this is not surprising. The nature of these sources remains uncertain. The increased emission might result from a narrow cone of beamed emission crosses our line of sight every few days. It is unclear, however, how a pulsed beam would lead to the distinctly asymmetric fast rise–slower decay profile. Alternatively, the flare might represent a period of rapid highly super-Eddington accretion onto a neutron star or stellar-mass black hole, perhaps during the periastron passage of a donor companion star in an eccentric orbit around a compact object. Such an explanation has been suggested to explain observed (albeit neutron star Eddington-limited) flares in galaxies^{1,24}. Finally, the high X-ray luminosity during the peak of the flare might represent accretion onto an intermediate-mass black hole. If the flares are Eddington-limited, black hole masses of 800 M_⊙ and 80 M_⊙ are implied for Sources 1 and 2, respectively, assuming a bolometric correction of 1.1 appropriate for a 2 keV disk blackbody temperature spectral model. The fast rise times constrain the maximum mass of a putative black hole, since the rise time cannot be shorter than the light travel time across the innermost stable circular orbit of the black hole. For both sources, the fastest rise happened over a 22 second period, implying an upper limit on the mass of a maximally-rotating black hole of 2×10^6 M_⊙. A black hole in this mass range is a particularly intriguing explanation for Source 2 if indeed its host is the stripped core of a dwarf galaxy.

References

- [1.] Sivakoff, G. R., Sarazin, C. L. & Jordán, A. Luminous X-Ray Flares from Low-Mass X-Ray Binary Candidates in the Early-Type Galaxy NGC 4697. *Astrophys. J.* 624, L17–L20 (2005).
- [2.] Tonry, J. L. et al. The SBF Survey of Galaxy Distances. IV. SBF Magnitudes, Colors, and Distances. *Astrophys. J.* 546, 681–693 (2001).
- [3.] Mei, S. et al. The ACS Virgo Cluster Survey. XIII. SBF Distance Catalog and the Three-dimensional Structure of the Virgo Cluster. *Astrophys. J.* 655, 144–162 (2007).
- [4.] Posson-Brown, J., Raychaudhury, S., Forman, W., Donnelly, R. H., & Jones, C. *Chandra* Observations of the X-Ray Point Source Population in NGC 4636. *Astrophys. J.* 695, 1094–1110 (2009).
- [5.] Dirsch, B., Schuberth, Y. & Richtler, T. A wide-field photometric study of the globular cluster system of NGC 4636. *Astron. Astrophys.* 433, 43–56 (2005).
- [6.] Schuberth, Y. et al. Dynamics of the NGC 4636 globular cluster system. An extremely dark matter dominated galaxy? *Astron. Astrophys.* 459, 391–406 (2006).
- [7.] Pandey, J. C. & Singh, K. P. A study of X-ray flares - II. RS CVn-type binaries. *Mon. Not. R. Astron. Soc.* 419, 1219–1237 (2012).
- [8.] Harris, G. L. H., Rejkuba, M. & Harris, W. E. The Distance to NGC 5128 (Centaurus A). *Publ. Astron. Soc. Australia* 27, 457–462 (2010).
- [9.] Harris, G. L. H., Geisler, D., Harris, H. C., & Hesser, J. E. Metal abundances from Washington photometry of globular clusters in NGC 5128. *Astron. J.* 104, 613–626 (1992).
- [10.] Woodley, K. A. et al. The Kinematics and Dynamics of the Globular Clusters and Planetary Nebulae of NGC 5128. *Astron. J.* 134, 494–510 (2007).
- [11.] Woodley, K. A. et al. Globular Clusters and X-Ray Point Sources in Centaurus A (NGC 5128). *Astrophys. J.* 682, 199–211 (2008).
- [12.] Mieske, S. et al. On central black holes in ultra-compact dwarf galaxies. *Astron. Astrophys.* 558, A14 (2013).
- [13.] Kouveliotou, C. et al. An X-ray pulsar with a superstrong magnetic field in the soft γ -ray repeater SGR1806-20. *Nature* 393, 235–237 (1998).
- [14.] Mereghetti, S. & Stella, L. The very low mass X-ray binary pulsars: A new class of sources? *Astrophys. J.* 442, L17–L20 (1995).
- [15.] Olive, J.-F. et al. Time-resolved X-Ray Spectral Modeling of an Intermediate Burst from SGR 1900+14 Observed by HETE-2 FREGATE and WXM. *Astrophys. J.* 616, 1148–1158 (2004).
- [16.] Kozlova, A. V. R. et al. The first observation of an intermediate flare from SGR 1935+2154. *Mon. Not. R. Astron. Soc.* 460, 2008 (2016).
- [17.] Younes, G. et al. Simultaneous NuSTAR/*Chandra* Observations of the Bursting Pulsar GRO J1744-28 during Its Third Reactivation. *Astrophys. J.* 804, 43 (2015).
- [18.] Cornlisse, R., Heise, J., Kuulkers, E., Verbunt, F., & in't Zand, J. J. M. The longest thermonuclear X-ray burst ever observed?. A BeppoSAX Wide Field Camera observation of 4U 1735-44. *Astron. Astrophys.* 357, L21–L24 (2000).
- [19.] Strohmayer, T. E. & Beown, E. F. A Remarkable 3 Hour Thermonuclear Burst from 4U 1820-30. *Astrophys. J.* 556, 1045–1059 (2002).
- [20.] Jonker, P. G. et al. Discovery of a New Kind of Explosive X-Ray Transient near M86. *Astrophys. J.* 779, 14 (2013).
- [21.] Luo, B., Brandt, W. N. & Bauer, F. Discovery of a fast X-ray transient in the *Chandra* Deep Field-South survey. *The Astronomers Telegram* 6541, 1 (2014).
- [22.] Glennie, A., Jonker, P. G., Fender, R. P., Nagayama, T., & Pretorius, M. L. Two fast X-ray transients in archival *Chandra* data. *Mon. Not. R. Astron. Soc.* 450, 3765–3770 (2015).
- [23.] Grimm, H.-J., Gilfanov, M. & Sunyaev, R. The Milky Way in X-rays for an outside observer. Log(N)-Log(S) and luminosity function of X-ray binaries from RXTE/ASM data. *Astron. Astrophys.* 391, 923–944 (2002).

[24.] Maccarone, T. J. An explanation for long flares from extragalactic globular cluster X-ray sources. *Mon. Not. R. Astron. Soc.* 364, 971–976 (2005).

Acknowledgments: We thank Tom Richtler for helpful discussions. J.A.I. was supported from *Chandra* grant AR6-17010X and NASA ADAP grant NNX10AE15G. G.R.S. acknowledges support of an NSERC Discovery Grant. A.J.R. was supported by the National Science Foundation grant AST-1515084. J.S. acknowledges support from NSF grants AST-1308124 and AST-1514763 and the Packard Foundation.

Author Contributions: J.A.I. led the *Chandra* data reduction and analysis, with contributions from W.P.M. for the *XMM-Newton* data reduction and analysis. T.S., I.P., and D.M. conducted the *Chandra* galaxy survey that yielded the two flare sources, with oversight from J.A.I. G.R.S., A.J.R., D.L., J.S., J.L., and J.M.M. contributed to the discussion and interpretation.

Competing Interests: The authors declare that they have no competing financial interests.

Correspondence: Correspondence and requests for materials should be addressed to J.A.I. (jairwin@ua.edu).

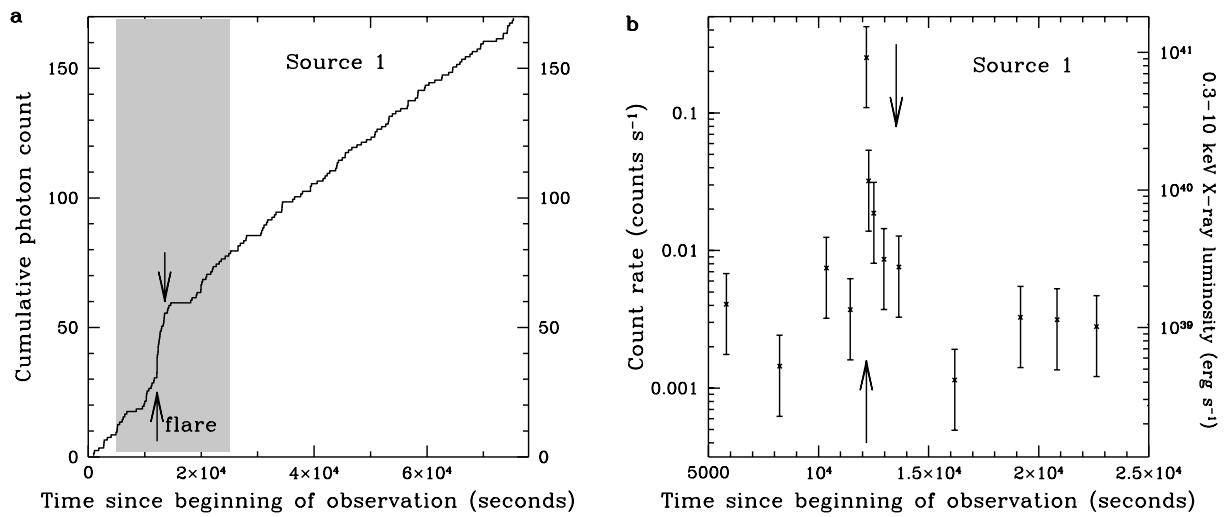


Figure 1 | The *Chandra* cumulative X-ray photon arrival time plot and light curve for Source 1 in the NGC 4636 globular cluster. a. In total, 162 photons were detected over the $\sim 76,000$ second observation. The flare began at the 12,000 second mark of the observation and lasted for 1,400 seconds. The beginning and ending of the flare are indicated by up and down arrows, respectively. **b.** Within the gray shaded region of the cumulative X-ray photon arrival time plot we derive the background-subtracted X-ray light curve. Each time bin contains five photons, with error bars representing the 1σ uncertainty expected from Poisson statistics.

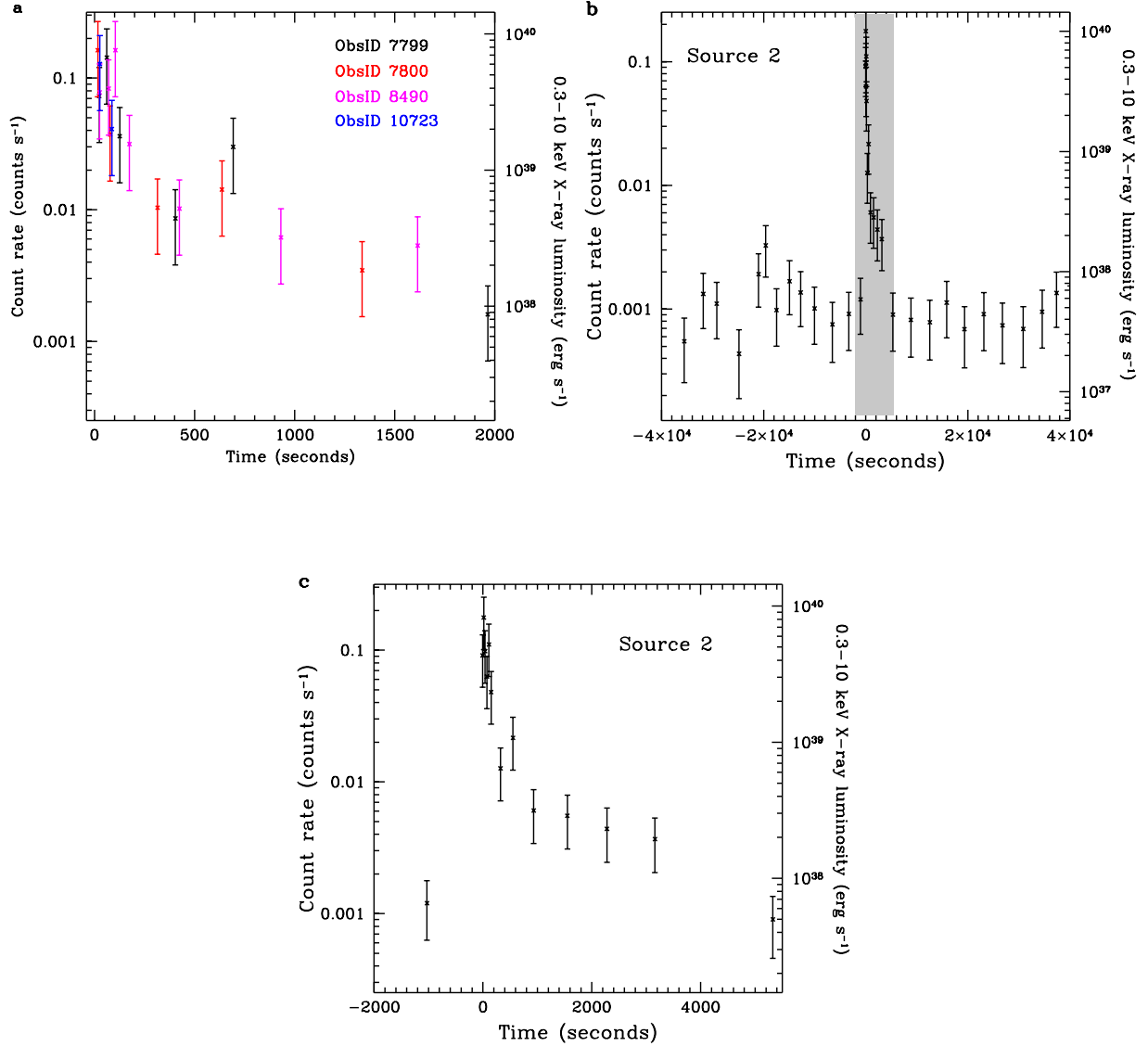


Figure 2 | Individual and combined background-subtracted X-ray light curves of Source 2 in the NGC 5128 globular cluster/ultracompact dwarf. a. The X-ray light curves for the four *Chandra* flares show similar behavior. Each time bin contains five photons, with 1σ uncertainties. b. The combined light curve of the four flares illustrates the fast rise/slow decay of the flares. Each time bin contains ten photons. c. Zooming in on the gray shaded region reveals that the luminosity during the flare rose quickly and remained steady in an ultraluminous state for ~ 200 seconds before decaying back to its persistent level after ~ 1 hour.

Methods

Flare Search Technique

We searched for flares from all point sources found in 70 *Chandra* observations of nearby luminous early-type galaxies. The *evt2* files were downloaded from the *Chandra* archive, and the source detection routine *wavdetect* in the Chandra Interactive Analysis of Observations (CIAO) package suite on the image files to create a list of sources detected at the $>3\sigma$ level. Our script then extracted the time-ordered photon arrival times for each source found by *wavdetect*. Next, our routines scanned the photon event list and searched for bursts by finding the time difference between each photon and the photon three photons forward in time from it (i.e., a 4-photon burst) and then calculated the Poisson probability of detecting that many photons over that time interval given the overall count rate of the source over the entire observation and the number of 4-photon burst trials present over the epoch. This was repeated for 5-photon bursts, 6-photon bursts, 7-photon bursts, etc., up to 20-photon bursts. If the probability of a burst of that magnitude from Poisson fluctuations was below our fiducial value (1 in 10^6) and the count rate during the N-photon burst was more than ten times the average count rate of the source over the observation the source was marked for further study. Note that our technique is more sophisticated than a simple KS-test on this distribution. Our technique found several flares from Milky Way M dwarf stars, both previously known and unknown, which were removed from consideration. Among the 7,745 sources detected in the 70 observations, Source 1 and Source 2 were the only non-Galactic sources not previously detected by other groups (which appear to be transients or one-time events^{20–22}) that were identified for which the random Poisson fluctuation probability was less than 10^{-6} , and for which peak-to-persistent count ratio exceeded ten (to exclude somewhat variable, but non-flaring sources).

Chandra and *XMM-Newton* Data Reduction

Those *Chandra* observations containing flares were then analyzed further using CIAO 4.7 with CALDB version 4.6.9. The sources exhibited flaring only in ObsIDs 3926 (for Source 1) and in ObsIDs 7799, 7800, 8490, and 10723 (for Source 2). The remaining three and 36 ObsIDs for Source 1 and Source 2, respectively, showed no flaring activity, did not have the source in the field of view of the detector, or the data were taken with a lower sensitivity detector (*Chandra* HRC/LETG/HETG) for which a flare of comparable intensity would not have been detected. Extended Data Table 1 lists all the searched *Chandra* and *XMM-Newton* observations of NGC 4636 and NGC 5128. The luminosity of the sources in the non-flare observations were consistent with the persistent luminosities of the sources during the flare observations. All flares occurred in ACIS-I pointings. The event lists were reprocessed using the latest calibration files at the time of analysis with the CIAO tool *chandra_repro*. None of the *Chandra* observations had any background flaring time intervals significant enough to warrant their removal considering we are interested in point sources. Energy channels below 0.3 keV and above 6.0 keV were ignored. Both Sources 1 and 2 were located at least $4'8''$ from the ACIS-I aim point in all the observations, so we used the CIAO tool *psfsize_srcs* to de-

termine the extraction radius for each observation that enclosed 90% of the source photons at an energy of 2.3 keV. All subsequent count rates and 0.3–10 keV X-ray luminosities were corrected for these point spread function (PSF) losses. Since each flare occurred at a large off-axis angle from the aim point, the photons were spread over a large PSF. Thus pile-up effects were negligible even at the peak of each flare. We do not believe there is any way for the flares to be an instrumental effect such as pixel flaring or cosmic ray afterglows, for which each recorded event during the flare would occur in a single detector pixel. Inspection of all the flare observations in detector coordinates revealed that the photons were not concentrated in a single detector pixel, but were instead spread out in detector space in accordance with the dither pattern of *Chandra* as would be expected from astrophysical photons. Furthermore, the photon energies of cosmic ray afterglows decrease with each successive photon which is not the case for the photons occurring during the flare.

While we did not conduct a survey of galaxies observed with *XMM-Newton*, we did utilize archival *XMM-Newton* data to search for additional flares from Source 1 and 2. The *XMM-Newton* observations for Source 1 did not reveal any detectable flaring behavior, but the 2014 February 9 (ObsID 0724060801) of Source 2 revealed a fifth flare for this source detected in both MOS1 and MOS2 detectors separately. To analyze the data, we used the 2014 November 4 release of the *XMM-Newton* Science Analysis Software (SAS), and the data were processed with the tool *emproc*, which filtered the data for the standard MOS event grades. Source 2 was only observed with the two MOS instruments, since it was not in the PN camera field of view (the observations used a restricted window due to the high count rate of the central AGN in NGC 5128). Periods of high background at the end of the observation were removed.

Cumulative Photon Arrival Time Plots for Sources 1 and 2

Each X-ray photon collected by *Chandra* or *XMM-Newton* is tagged with a position, energy, and time of arrival, allowing a photon-by-photon account of each X-ray source at a time resolution set by the read-out time for the detector (3.1 seconds for *Chandra* ACIS-I and 2.6 seconds for *XMM-Newton* EPIC MOS). Cumulative photon arrival time plots are a simple way to observe time variability over the course of the observation. While a source with constant flux will yield a cumulative photon arrival time plot with a constant slope, a flare will appear as a nearly vertical rise in the plot as photons stream in over a short period of time. Figure 1 shows the cumulative photon arrival time plot for Source 1, illustrating the onset of the flare around the 12,000 second mark following the beginning of the observation.

The cumulative photon arrival time plot from each of the five flares from Source 2 is shown in Extended Data Figure 1. In each plot the beginning of the flare is evident. The final *Chandra* flare (ObsID 10723) occurred just at the end of this short observation. The persistent count rate within the $10''$ source extraction region of the *XMM-Newton* observation is compromised by background, but the onset of the flare at the 16,000 second mark is evident.

Peak Flare Rate and the Statistical Significance of the Flares

We estimated the peak flare rate of Source 1 based on the arrival times of the first six photons of the flare, which arrived over a 22 second period. Given the uncertainty in when the peak ended, we neglect the sixth photon of the flare to conservatively estimate a count rate of $0.25_{-0.11}^{+0.17}$ counts s^{-1} (1σ uncertainty) after correcting for the 10% of emission expected to be scattered out of the source extraction region due to PSF losses. Background was negligible during the flare, and accounted for only 7% of the emission inside the source extraction region during persistent times.

Since Source 1 only flared once, it is necessary to determine accurately how many independent trials were contained in the sources searched within our sample of galaxies to determine the likelihood that the flare could result from a random fluctuation in the persistent count rate. The two sources discussed here were found as part of a 70 observation sample observed with *Chandra* composed primarily of large elliptical galaxies at distances of 20 Mpc and closer, with a majority of the galaxies residing in Virgo or Fornax. Within these 70 observations, 7,745 sources were detected yielding a total of 8.5×10^5 photons. This is equivalent to 1.7×10^5 independent 5-photon groupings. Statistically, the chance of detecting five or more photons in 22 seconds for a source that normally emits at 1.9×10^{-3} counts s^{-1} (the count rate in the persistent state before correcting for PSF losses) is 1.0×10^{-9} . With 1.7×10^5 independent trials throughout our sample, the chance of finding a single 5-photon burst for the Source 1 flare is 1.7×10^{-4} . Searching over multiple photon burst scales increases the odds of finding a chance statistical fluctuation. A previous study¹ performing a similar calculation has calculated this correction factor to be ~ 2.5 using Monte Carlo simulations, so we apply that correction here leading to a false detection rate of 4.3×10^{-4} . A similar exercise for the entire burst (25 photons in 1,400 seconds) leads to a chance fluctuation probability of 6.4×10^{-6} .

A similar exercise can be performed for each flare detected in Source 2 by *Chandra* observations. In each case, the flare at its peak was detected using nine photons in 51 seconds, six photons in 22 seconds, seven photons in 22 seconds, and six photons in 37 seconds, respectively. Given the persistent count rates in each observation, and correcting appropriately for both the number of independent 9-photon, 6-photon, and 7-photon trials (i.e., scaling appropriately from the 1.7×10^5 independent 5-photon trials) and the multi-burst search correction factor of 2.5, we calculate probabilities of 1.4×10^{-5} , 7.1×10^{-7} , 1.2×10^{-6} , and 9.0×10^{-4} of a false flare detection for each flare, respectively. Since we only considered *XMM-Newton* data after having detected the flares in the *Chandra* data, the probability that the flare observed with *XMM-Newton* was falsely detected is 5.0×10^{-8} given the 113,000 seconds of total exposure on this source. When combined this gives a probability that all the flares were falsely detected is 5.4×10^{-28} .

X-ray Light Curves

Owing to the limited photon statistics for the flare in Source 1, only a crude X-ray light curve was obtained by binning photons in groups of five and determining the count rate over which

the five photons were collected (Figure 1). The four individual 5-photon bin *Chandra* light curves for Source 2 showed similar timing behavior (Figure 2), which gave us confidence to combine them into one light curve. For each flare, we determined the average arrival time of the first three photons of the flare and set this to ‘time zero’. Thus, photons before the flare were assigned a negative time value. The four photon lists were then combined at ‘time zero’ to provide a combined photon list. Photons were then binned in groups of ten to calculate count rates during the time period over which the ten photons were collected. The count rates were divided by four to give the average count rate per time bin per flare. Since the fourth *Chandra* epoch (ObsID 10723) was very short and does not extend from $-40,000$ seconds to $40,000$ seconds from the start of the flare, we corrected the count rate accordingly to account for the temporal coverage of this epoch. The count rates were corrected for the loss of photons outside the extraction region due to the PSF, and for the expected background (while negligible during the flare, this accounted for 14% of the emission during persistent periods). The combined light curve for Source 2 is shown in Figure 2. A sharp rise at the beginning of the flare was followed by a flat ultraluminous state for ~ 200 seconds. The improvement in statistics by combining the four light curves traces the duration of the decay in flux out to $\sim 4,000$ seconds. Following the flare, the count rate of the source was remarkably consistent with the pre-flare count rate.

Spectral Fitting and Source Luminosities

For Source 1, we extracted a combined spectrum during the pre- and post-flare period using the CIAO tool *specextract*. Background was collected from a source-free region surrounding our source. Using XSPECv12.8, a power law model absorbed by the Galactic column density in the direction of NGC 4636 ($N_H = 1.8 \times 10^{20}$ cm^{-2})²⁵ using the TBABS absorption model was employed to fit the background-subtracted spectrum. Only energy channels over the range 0.5–6.0 keV were considered in the fit. The spectrum was grouped to contain at least one count per channel and the C-statistic was used in the fit. A best-fit power law photon index of 1.6 ± 0.3 (90% uncertainty) was found. This fit implies an unabsorbed luminosity of $7.9 \pm 0.8 \times 10^{38}$ erg s^{-1} during the persistent state (all reported luminosities below have also been corrected for absorption). Since the flare period contained only 25 photons, the flare spectrum was poorly well-constrained ($\Gamma = 1.6 \pm 0.7$). This led to a peak luminosity during the first 22 seconds of the flare of $9_{-4}^{+6} \times 10^{40}$ erg s^{-1} , a factor of ~ 120 greater than during persistent periods combined. Freeing the absorption did not substantially change the fit. Fitting the flare with a disk blackbody model gave a slightly worse fit with $kT_{\text{blackbody}} = 1.3_{-0.5}^{+2.0}$ keV and a luminosity 30% less than the power law fit.

For Source 2, we combined the spectra from the flare periods of the four *Chandra* observations using *specextract* into one spectrum. The same was done for the pre- and post-flare periods combined. The best-fit power law photon indices for persistent and flare periods assuming a Galactic column density in the direction of NGC 5128 (8.6×10^{20} cm^{-2})²⁵ were 1.0 ± 0.2 and 1.2 ± 0.3 (90% uncertainty), respectively. Again,

this indicates no significant change in the spectral shape during the flare. These spectral models implied persistent and peak flare luminosities of $4.4 \pm 0.3 \times 10^{37}$ erg s⁻¹ and $8.1_{-2.5}^{+3.5} \times 10^{39}$ erg s⁻¹, respectively, an increase of ~ 200 in less than a minute. When we split the flare period into the flat ultraluminous (first 200 seconds) and decay times (200–4,000 seconds), we also found no significant spectral evolution. We allowed the Galactic column density N_H to vary in the fits and found a somewhat softer photon index ($\Gamma = 1.6 \pm 0.6$ in the persistent state and $\Gamma = 1.3 \pm 0.7$ during the flare) with $N_H = 6_{-4}^{+5} \times 10^{21}$ cm⁻² for the persistent state and unconstrained below 5×10^{21} cm⁻² during the flare (90% uncertainties for two interesting parameters). In both instances, freeing the absorption only changed the unabsorbed L_X by $< 10\%$. The source does not reside in the dust lane of NGC 5128, so this excess absorption, if real, might be intrinsic to the source. We also fitted the flare spectrum with a disk blackbody model with fixed N_H at the Galactic value and found a best-fit temperature of $2.2_{-0.6}^{+1.7}$ keV, with a comparable goodness-of-fit to that of the power law model and a luminosity 20% below that derived from the power law fit.

For the *XMM-Newton* observation, the spectrum and response files were generated using the standard SAS tasks *evselect*, *backscale*, *arfgen*, and *rmfgen*. Since the count rate during the pre- and post-flare time period is dominated by background (owing to the much larger extraction region compared to *Chandra* and higher background rates), we did not extract a spectrum for the persistent period. We extracted the background-subtracted flare spectrum in a 30'' region around the source and fitted it with the absorbed power law described above for *Chandra* observations. The slope of the power law was poorly-constrained ($\Gamma = 1.5 \pm 0.5$) owing to the low number of photons detected in the flare, but the slope was consistent with the fit from the co-added *Chandra* spectrum. The peak luminosity of the flare was $1.6_{-0.7}^{+1.1} \times 10^{40}$ erg s⁻¹, again consistent with the *Chandra* flares.

Probability of the Flare and Persistent Emission Being From Two Different Sources

We have assumed that the persistent and flare emission emanate from a single source within the globular cluster hosts of Sources 1 and 2, but it is possible that two separate sources in the same cluster are responsible for the emission. The probability that a globular cluster hosts an X-ray binary of a particular X-ray luminosity depends on the luminosity of the source²⁶, as well as the properties of the globular cluster such as its mass, concentration, and metal abundance^{27,28}. From previous work²⁷, the number of X-ray sources more luminous than 3.2×10^{38} erg s⁻¹ in a globular cluster that has a mass M , stellar encounter rate Γ_h , half-light radius r_h , and cluster metallicity Z is $0.041 \left(\frac{\Gamma_h}{10^7}\right)^{0.82 \pm 0.05} \left(\frac{Z}{Z_\odot}\right)^{0.39 \pm 0.07}$, where $\Gamma_h = \left(\left(\frac{M}{M_\odot}\right) \frac{1}{2\pi}\right)^{3/2} \left(\frac{r_h}{1 \text{ pc}}\right)^{-5/2}$.

The globular cluster hosting Source 1 has photometry in Kron-Cousins R -band and Washington C filters; $R = 23.02$ and $C - R = 1.94$. This color corresponds to a photometrically derived metallicity of $Z/H = -0.08$ dex ($Z = 0.8 Z_\odot$)²⁹. Using a single population model³⁰ given a Kroupa initial mass

function, 13 Gyr age, and $Z/H = -0.08$ dex, an M/L of 4.1 in R -band is expected for this cluster. Given the distance to NGC 4636 ($d = 14.3$ Mpc), the R -band M/L referenced above, and $M_{R,\odot} = 4.42$, we estimate a globular cluster mass of $3.0 \times 10^5 M_\odot$. Since we have no size measurement for this globular cluster, we conservatively estimate a minimum size of 1.5 pc, which is the 3σ lower limit based on a survey of globular clusters in the Virgo cluster³¹. With these values, we estimate the globular cluster is expected to have 0.017 X-ray binaries above 3.2×10^{38} erg s⁻¹. To determine the number of X-ray binaries expected above the observed persistent X-ray luminosity of Source 1, we apply the X-ray luminosity function in globular clusters found in a previous study²⁶, which predicts that the Source 1 persistent luminosity (8×10^{38} erg s⁻¹) is ten times less likely to be found in a globular cluster than a 3.2×10^{38} erg s⁻¹ source. This leads to an estimate of 0.0017 X-ray sources equal to or more luminous than Source 1. Thus, after having found a flaring source, the probability that the persistent emission comes from a different X-ray binary in this cluster is $< 0.17\%$. If we conservatively assume that the predicted number of LMXBs could be 50% higher (approximately convolving all of the uncertainty sources), the probability is $< 0.24\%$.

The globular cluster/ultracompact dwarf galaxy hosting Source 2 has a spectroscopically-determined metallicity of $Z/H = -0.85$ dex ($Z = 0.14 Z_\odot$)³². The derived stellar mass¹² of the source is $3.1 \times 10^6 M_\odot$. Given its size¹² of 7 pc, and correcting for the luminosity function²⁶ (which predicts that a 4×10^{37} erg s⁻¹ source is ten times more likely to be found in a globular cluster than a 3.2×10^{38} erg s⁻¹ source), we estimate the globular cluster is expected to have 0.064 X-ray binaries above 4×10^{37} erg s⁻¹. Thus after having found a flaring source, the probability that the persistent emission comes from a different X-ray binary in this cluster is $< 6.4\%$. If we conservatively assume that the predicted number of LMXBs could be 50% higher (approximately convolving all of the uncertainty sources), the probability is $< 9.1\%$. We note that this might be an overestimate given that ultracompact dwarfs appear to harbor X-ray sources at a lower rate than globular clusters³³.

Even in the most conservative case, the combined probability that both sources arise from different sources than the persistently emitting sources is $< 1.5 \times 10^{-4}$.

For both sources, we determined the position of the sources separately during its flare phase and persistent phase and found no statistical difference within the positional uncertainties. This is not highly constraining, however, given the large PSF of *Chandra* at the off-axis location of the flares.

Code availability: The code to find X-ray flares is available at <http://pages.astronomy.ua.edu/jairwin/software/>.

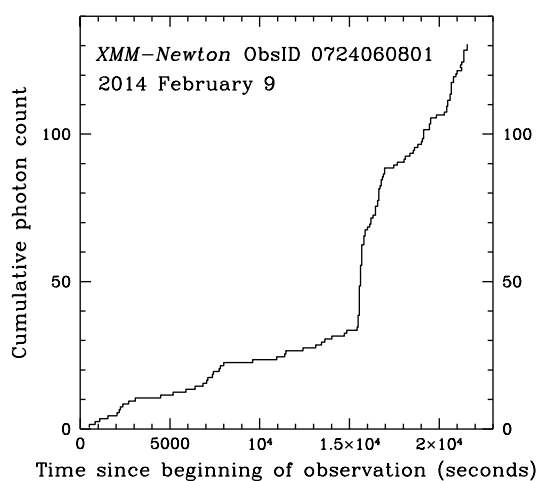
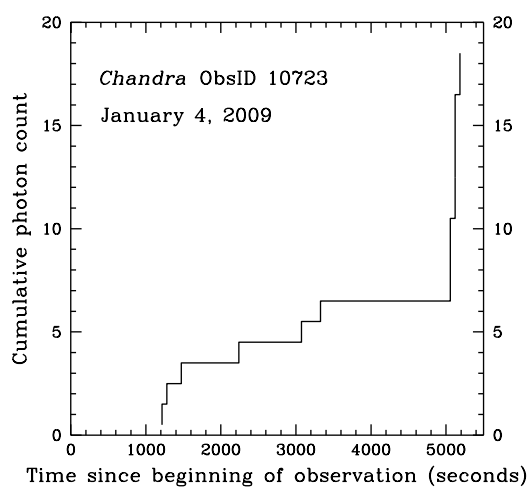
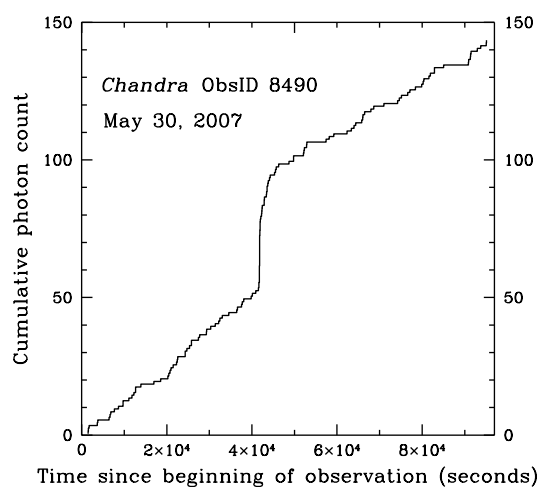
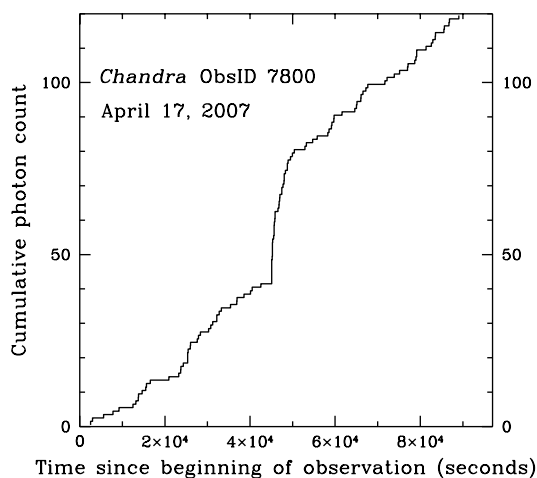
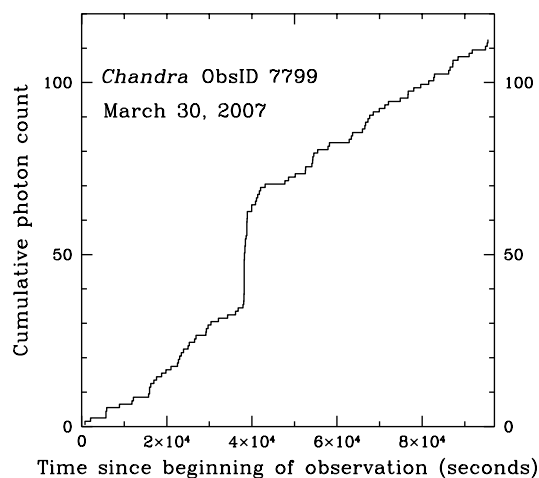
References

- [25.] Dickey, J. M. & Lockman, F. J. H I in the Galaxy. *Annu. Rev. Astron. Astrophys.* 28, 215–261 (1990).
- [26.] Zhang, Z. et al. Luminosity functions of LMXBs in different stellar environments. *Mon. Not. R. Astron. Soc.* 533, A33 (2011).
- [27.] Sivakoff, G. R. et al. The Low-Mass X-Ray Binary and Globular Cluster Connection in Virgo Cluster Early-Type Galax-

- ies: Optical Properties. *Astrophys. J.* 660, 1246–1263 (2007).
- [28.] Kundu, A., Maccarone, T. J. & Zepf, S. E. Probing the Formation of Low-Mass X-Ray Binaries in Globular Clusters and the Field. *Astrophys. J.* 662, 525–543 (2007).
- [29.] Harris, W. E. & Harris, G. L. H. The Halo Stars in NGC 5128. III. An Inner Halo Field and the Metallicity Distribution. *Astron. J.* 123, 3108–3123 (2002).
- [30.] Maraston, C. Evolutionary population synthesis: models, analysis of the ingredients and application to high- z galaxies. *Mon. Not. R. Astron. Soc.* 362, 799–825 (2005).
- [31.] Jórđan, A. et al. The ACS Virgo Cluster Survey. X. Half-Light Radii of Globular Clusters in Early-Type Galaxies: Environmental Dependencies and a Standard Ruler for Distance Estimation. *Astrophys. J.* 634, 1002–1019 (2005).
- [32.] Beasley, M. A. et al. A 2dF spectroscopic study of globular clusters in NGC 5128: probing the formation history of the nearest giant elliptical. *Mon. Not. R. Astron. Soc.* 386, 1443–1463 (2008).
- [33.] Pandya, V., Mulchaey, J. & Greene, J. E. A Comprehensive Archival Chandra Search for X-Ray Emission from Ultra-compact Dwarf Galaxies. *Astrophys. J.* 819, 162 (2016).

Source	Telescope/Detector	ObsID	Observation Date	Exposure (ksec)	Flare?
1	<i>Chandra</i> /ACIS-I	324	1999-12-04	8.5	N
1	<i>Chandra</i> /ACIS-S	323	2000-01-26	53.1	N
1	<i>XMM-Newton</i> /EPIC	0111190101	2000-07-13	27.2	N
1	<i>XMM-Newton</i> /EPIC	0111190501	2000-07-13	6.6	N
1	<i>XMM-Newton</i> /EPIC	0111190201	2000-07-13	66.3	N
1	<i>XMM-Newton</i> /EPIC	0111190701	2001-01-05	64.4	N
1	<i>Chandra</i> /ACIS-I	3926	2003-02-15	75.7	Y
1	<i>Chandra</i> /ACIS-I	4415	2003-02-15	75.3	N
2	<i>Chandra</i> /HRC-I	463	1999-09-10	19.7	N
2	<i>Chandra</i> /HRC-I	1253	1999-09-10	6.9	N
2	<i>Chandra</i> /ACIS-I	316	1999-12-05	36.2	...
2	<i>Chandra</i> /HRC-I	1412	1999-12-21	15.1	N
2	<i>Chandra</i> /HRC-I	806	2000-01-23	65.3	N
2	<i>Chandra</i> /ACIS-I	962	2000-05-17	37.0	N
2	<i>XMM-Newton</i> /EPIC	0093650201	2001-02-02	23.9	N
2	<i>Chandra</i> /ACIS-S/HETG	1600	2001-05-09	47.5	N
2	<i>Chandra</i> /ACIS-S/HETG	1601	2001-05-21	52.2	N
2	<i>XMM-Newton</i> /EPIC	0093650301	2002-02-06	15.3	N
2	<i>Chandra</i> /ACIS-S	2978	2002-09-03	45.2	...
2	<i>Chandra</i> /ACIS-S	3965	2003-09-14	50.2	...
2	<i>Chandra</i> /ACIS-I	7797	2007-03-22	98.2	N
2	<i>Chandra</i> /ACIS-I	7798	2007-03-27	92.0	N
2	<i>Chandra</i> /ACIS-I	7799	2007-03-30	96.0	Y
2	<i>Chandra</i> /ACIS-I	7800	2007-04-17	92.1	Y
2	<i>Chandra</i> /ACIS-I	8489	2007-05-08	95.2	N
2	<i>Chandra</i> /ACIS-I	8490	2007-05-30	95.7	Y
2	<i>Chandra</i> /ACIS-I	10723	2009-01-04	5.2	Y
2	<i>Chandra</i> /ACIS-I	10724	2009-03-07	5.2	N
2	<i>Chandra</i> /HRC-I	10407	2009-04-04	15.2	N
2	<i>Chandra</i> /ACIS-I	10725	2009-04-26	5.0	N
2	<i>Chandra</i> /ACIS-I	10726	2009-06-21	5.2	N
2	<i>Chandra</i> /ACIS-S	10722	2009-09-08	50.0	...
2	<i>Chandra</i> /HRC-I	10408	2009-09-14	15.2	N
2	<i>Chandra</i> /ACIS-I	11846	2010-04-26	4.8	N
2	<i>Chandra</i> /ACIS-I	11847	2010-09-16	5.1	...
2	<i>Chandra</i> /ACIS-I	12155	2010-12-22	5.1	N
2	<i>Chandra</i> /ACIS-I	12156	2011-06-22	5.1	N
2	<i>Chandra</i> /ACIS-I	13303	2012-04-14	5.6	N
2	<i>Chandra</i> /ACIS-I	13304	2012-08-29	5.1	N
2	<i>Chandra</i> /ACIS-I	15294	2013-04-05	5.1	N
2	<i>XMM-Newton</i> /EPIC	0724060501	2013-07-12	12.0	N
2	<i>XMM-Newton</i> /EPIC	0724060601	2013-08-07	12.0	N
2	<i>Chandra</i> /ACIS-I	15295	2013-08-31	5.4	N
2	<i>XMM-Newton</i> /EPIC	0724060701	2014-01-06	26.5	N
2	<i>XMM-Newton</i> /EPIC	0724060801	2014-02-09	23.4	Y
2	<i>Chandra</i> /ACIS-I	16276	2014-04-24	5.1	N
2	<i>Chandra</i> /ACIS-I	16277	2014-09-08	5.4	...
2	<i>Chandra</i> /ACIS-I	17471	2015-03-14	5.4	N
2	<i>Chandra</i> /ACIS-S/LETG	17147	2015-05-13	49.7	N
2	<i>Chandra</i> /ACIS-S/LETG	17657	2015-05-17	50.4	N

Extended Data Table 1: Summary of the *Chandra* and *XMM-Newton* Observations of Source 1 and 2



Extended Data Figure 1: The cumulative X-ray photon arrival time plots for the five flares of Source 2 in NGC 5128. The first four flares were observed by *Chandra* with the fifth flare by *XMM-Newton*. In ObsID 10723, the first photon of the observation was not received until 1100 seconds after the observation began, and the observation ended mid-flare.